doi:10.1017/S1431927621000891
Microsc. Microanal. 27 (Suppl 1), 2021

Local computational methods to improve the interpretability and analysis of cryo-EM maps

Satinder Kaur[1], Josue Gomez-Blanco[2], Ahmad A. Z. Khalifa[1], Swathi Adinarayanan[1], Ruben Sanchez-Garcia[3], Daniel Wrapp[4], Jason McLellan[3], Khanh Huy Bui[1] and Javier Vargas[5]

[1]Department of Anatomy and Cell Biology, McGill University 3640 Rue University, Montréal, QC, Canada, United States, [2]Universidad Complutense de Madrid, United States, [3]United States, [4]Department of Molecular Biosciences, The University of Texas at Austin, Austin, TX, USA, Hanover, New Hampshire, United States, [5]Departmento de Óptica, Universidad Complutense de Madrid, Madrid, Spain, United States

High-resolution cryo-electron microscopy (cryo-EM) maps help to visualize and analyze biological macromolecules in their native state as well as to understand their biological functions[1]. Density contrast is as important as a resolution to interpret these maps. Contrast lost at high-resolution in cryo-EM maps results from a resolution-dependent amplitude-falloff, typically called as B-factor. B-factor sharpening approaches[2–4] allow regaining the lost contrast in the maps. Additionally, effective B-factors help to recognize important map issues such as loss of resolution by macromolecular flexibility, molecular drifting due to charging effects, or possible errors in the reconstruction workflow[4–6]. However, the application of a uniform B-factor for map sharpening to reconstructions showing heterogenous B-factor distributions can lead to 'over sharpening'. In this case, cryo-EM maps are usually distorted and show broken destinies and noise boosting, which may affect the final *ab initio* modeling. Another important local parameter that was not available yet for cryo-EM map analysis is the map local occupancy, which estimates the presence of an atom at its mean position.

Here, we introduce semi-automated procedures to i) prevent the map distortions while improving the cryo-EM map interpretability at high resolution; ii) attain local B-factors and electron density occupancy maps. The desired outcome of all procedures is to improve the map contrast and propose new local metrics (local B-factor and occupancy map) for improving the interpretation and visibility of cryo-EM reconstruction. The only input requirements are the binary solvent mask, a resolution range, and the map to enhance or analyze.

The proposed approaches are called LocSpiral, LocBSharpen, LocBFactor and LocOccupancy[7] and have in common the usage of the spiral phase transformation, which can determine the modulation or amplitude map at a different resolution for cryo-EM reconstruction. Specifically, our local map enhancement approach, called LocSpiral, can strongly improve the interpretation and visibility for maps affected by the heterogeneous distribution of local resolutions/SNRs, as shown in several publications[1-4]. During our studies of type IV pili, we discovered nanotube like structures correlated with heterologous expression of the *Pseudomonas aeruginosa* major type IV pilin, PilA, in some *Escherichia coli* strains. We have coined these membranous tubular structures P-pods for pilin-induced pods based partly on their appearance in negative stain transmission electron microscopy images. Biochemical analysis showed that the major protein inside of P-pods is the inner membrane protein PilA. Because some membranous appendages serve as transport tunnels, we tested horizontal gene transfer in the P-pods; these studies revealed that P-pods are unable to transfer plasmid DNA.

To further characterize the structure of P-pods we carried out both negative stain TEM imaging and cryo-electron tomography. The cells were incubated on LB agar with inducers for 16 hours. Cells were resuspended in LB liquid medium to an OD_{600} = 0.01 and spotted on to glow-discharged, Quantifoil R2/1 mesh, gold grids (Quantifoil, Germany) with 5 nm carbon coating, in a humified chamber for 3.5 hours. Three mL of BSA-treated 10 nm colloidal gold (Electron Microscopy Sciences, USA) was applied onto the grids and then plunge-frozen in liquid ethane using a Leica EM GP (Leica Microsystems, Germany). Data collection was performed on a Titan Krios (Thermo Scientific, USA) FEG TEM operated at 300 kV and equipped with a Gatan K3 direct electron detector and a Gatan

bioquantum energy filter, at the University of Wisconsin-Madison Cryo-EM Research Center. Images were acquired with a pixel size of 0.4603 nm on the specimen and a total electron does between 120 to 130 $e^-/Å^2$. Data were collected at 2° increments from -60° to +60° (61 images) with a nominal defocus range of -4.0 to -6.0 µm to enhance contrast of various cell components. Tilt series images were collected using SerialEM [5]. Tomographic reconstructions were generated using IMOD [6] following tilt-series image motion correction by motioncor2 [7] and data were binned two-fold during this process. Neural network based tomogram segmentation models of P-pods were produced with EMAN2 [8].

The resulting 3D reconstructions revealed that P-pods originate at the inner membrane and P-pod extrusion may occur in multiple ways (Figure 1). P-pods may exit the cells through breaks in the outer membrane or by blebbing of the outer membrane which eventually ruptures and releases P-pods (Figure 1). Also, our data indicates that P-pods are comprised of a single lipid-bilayer, do not transport other vesicles, and are typically observed as a string of segmented vesicles once outside of the cell (Figure 2). Correlative light and electron microscopy (CLEM) could provide additional evidence for the localization of PilA within the cell and P-pods and may be the focus of follow up experiments. The biochemical and structural studies presented here reveal that, though similar to nanotubes, P-pods are novel membranous extracellular appendages that spontaneously assemble as the result of PilA over-expression in *E. coli* and may be a result of protein crowding that leads to positive membrane curvature of the inner membrane.

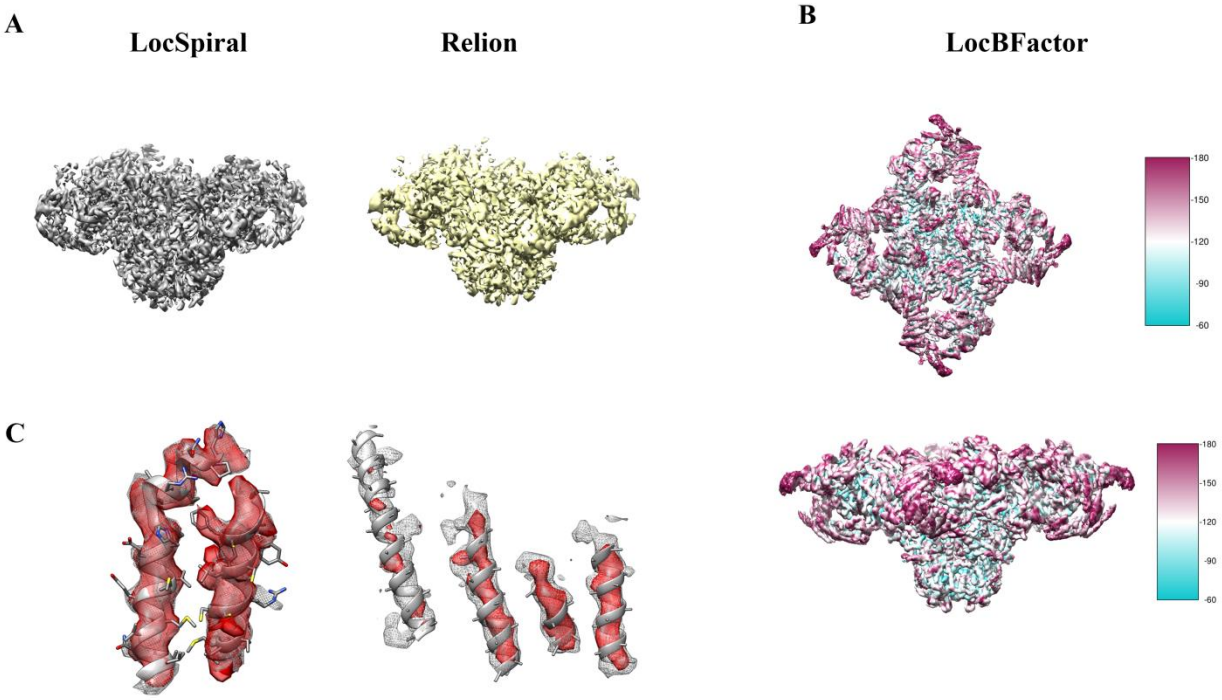

Figure 1. Characterization of P-pod extrusion via blebbing or membrane breach. A) Tomogram reconstruction of an E. coli cell expressing P. aeruginosa PilA protein resulting in blebbing of the outer membrane and localization of p-pods to the bleb. B) Tomogram reconstruction of the PilA expression system resulting in breaks along the outer membrane which allow for extrusion of p-pods. Figures represent a central slice with a thickness of 4.6 nm.

https://doi.org/10.1017/S1431927621000891 Published online by Cambridge University Press

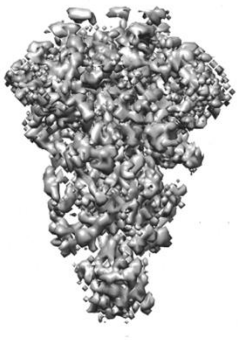

Figure 2. Extracellular P-pod structures. A) Tomogram reconstruction of extracellular p-pods as a string of segmented vesicles and B) a magnified view of a p-pod segment. Figures represent a central slice with a thickness of 4.6 nm.

References

1. Pal, R.R., et al., *Pathogenic E. coli Extracts Nutrients from Infected Host Cells Utilizing Injectisome Components.* Cell, 2019. **177**(3): p. 683-696.e18.
2. Weiner, J.H., et al., *Overproduction of fumarate reductase in Escherichia coli induces a novel intracellular lipid-protein organelle.* J Bacteriol, 1984. **158**(2): p. 590-6.
3. Shetty, A., et al., *Nanopods: a new bacterial structure and mechanism for deployment of outer membrane vesicles.* PloS one, 2011. **6**(6): p. e20725-e20725.
4. Wang, F., et al., *Structure of Microbial Nanowires Reveals Stacked Hemes that Transport Electrons over Micrometers.* Cell, 2019. **177**(2): p. 361-369.e10.
5. Mastronarde, D.N., *Automated electron microscope tomography using robust prediction of specimen movements.* Journal of Structural Biology, 2005. **152**(1): p. 36-51.
6. Kremer, J.R., D.N. Mastronarde, and J.R. McIntosh, *Computer Visualization of Three-Dimensional Image Data Using IMOD.* Journal of Structural Biology, 1996. **116**(1): p. 71-76.
7. Zheng, S.Q., et al., *MotionCor2: anisotropic correction of beam-induced motion for improved cryo-electron microscopy.* Nature methods, 2017. **14**(4): p. 331-332.
8. Chen, M., et al., *Convolutional neural networks for automated annotation of cellular cryo-electron tomograms.* Nature methods, 2017. **14**(10): p. 983-985.
9. This research was supported by funds from the University of Wisconsin-Madison, National Institutes of Health (R01GM104540 and R01GM104540-03S1) to E.R.W. J.C.S. was supported in part by the Biotechnology Training Program, T32GM135066. All EM data was collected at the University of Wisconsin-Madison, Department of Biochemistry Cryo-EM Research Center. The authors gratefully acknowledge use of facilities and instrumentation at the UW-Madison Wisconsin Centers for Nanoscale Technology (wcnt.wisc.edu) partially supported by the NSF through the University of Wisconsin Materials Research Science and Engineering Center (DMR-1720415).